Journal of Materials Chemistry

Cite this: *J. Mater. Chem.*, 2012, **22**, 1662

www.rsc.org/materials

**PAPER**

# Superparamagnetic cellulose fiber networks *via* nanocomposite functionalization

**Despina Fragouli,*[a] Ilker S. Bayer,[a] Riccardo Di Corato,[b] Rosaria Brescia,[b] Giovanni Bertoni,[bc] Claudia Innocenti,[d] Dante Gatteschi,[d] Teresa Pellegrino,[b] Roberto Cingolani[b] and Athanassia Athanassiou[ab]**

***Received 23rd September 2011, Accepted 4th November 2011***
**DOI: 10.1039/c1jm14755b**



We present a simple and cost-effective method for rendering networks of cellulose fibers, such as paper, fabrics or membranes, superparamagnetic by impregnating the individual fibers with a reactive acrylic monomer. The cellulose fibers are wetted by a cyanoacrylate monomer solution containing superparamagnetic manganese ferrite colloidal nanoparticles. Upon moisture initiated polymerization of the monomer on the fiber surfaces, a thin nanocomposite shell forms around each fiber. The nanocomposite coating renders the cellulose fibers water repellent and magnetically responsive. Magnetic and microscopy studies prove that the amount of the entrapped nanoparticles in the nanocomposite shell is fully controllable, and that the magnetic response is directly proportional to this amount. A broad range of applications can be envisioned for waterproof magnetic cellulose materials (such as magnetic paper/tissues) obtained by such a simple yet highly efficient method.

## 1. Introduction

Cellulose is the main structural component of various plants and the most abundant material on earth. Various natural derivatives, such as cotton and wood, are mainly composed of cellulose fibers and are widely used for everyday life applications. In particular, they are utilized as natural fibers, fabrics, pulps, papers, and wooden structures. Recently, cellulose fiber networks have been receiving much attention, since they are important candidates for the development of low cost functional devices such as sensors,[1,2] actuators,[3] transistors,[4] energy storage devices,[5] MEMS[6] or lab-on-paper devices.[7,8] Therefore, rendering cellulosic fibers multifunctional by using nanostructured materials is of great importance. Specifically, their functionalization with magnetic nanoparticles (NPs) makes them suitable for important applications, such as security tags on paper, magnetic actuators, electromagnetic shielding materials, magnetographic printing, *etc.* For this scope, various techniques have been used, such as lumen loading,[9–11] direct wet end addition,[12] fiber nanocoating[13] or *in situ* synthesis of NPs on the fibers,[14–16] mostly applied during the fabrication procedure of the cellulosic network product. This makes the application range pretty limited, but most importantly these methods reveal various drawbacks like complicated preparation procedures,[14,16] loss of mechanical properties, or reduced magnetic response.[12] Following a different approach, a recent study showed that by using commercial cellulose paper, magnetic microactuators can be formed. This was obtained by wetting the cellulose fibers with a ferrofluid, and it was shown that the nanofillers impregnated the intrafiber pores by forming a magnetic layer, while for water resistivity it was necessary to cover the cellulosic paper surface with polymer layers.[3]

Herein we propose an alternative, single step, low cost, and post-production scalable method for the formation of hydrophobic superparamagnetic nanocomposite cellulose networks. The cellulose sheets are modified in the post-production phase, by dip coating in a nanocomposite solution consisting of superparamagnetic colloidal NPs and a cyanoacrylate (CA) monomer. The monomer is polymerized naturally around each fiber, forming a 3-D soft magnetic hydrophobic shell, without changing the overall physical characteristics of the sample (size and shape). These nanocomposite shells around the cellulose fibers render the cellulose sheet water repellent and superparamagnetic at the same time. The proposed method can be applied to many various types of commercial cellulosic fiber networks such as paper, fabrics or membranes, eliminating the necessity to modify the standard production process of the pulp or fibers.

## 2. Experimental

### 2.1 Materials

Whatman Type-1 cellulose sheets were used in all experiments. This product is chemically pure and free from silicones or other

[a]*Center for Biomolecular Nanotechnologies @UNILE, Istituto Italiano di Tecnologia, via Barsanti, 73010 Arnesano, LE, Italy. E-mail: despina.fragouli@iit.it; Tel: +39 0832 295719*
[b]*Istituto Italiano di Tecnologia (IIT), via Morego 30, 16163 Genova, Italy*
[c]*IMEM-CNR, Parco Area delle Scienze 37/A, 43124 Parma, Italy*
[d]*INSTM-RU of Florence and Department of Chemistry, University of Florence, via della Lastruccia 3-13, 50019 Sesto F.no, Firenze, Italy*

additives. No chemical or physical pre-treatment was applied to the sheets before the experiments. Ethyl-2-cyanoacrylate (ECA) monomer was procured from Sigma-Aldrich. Reagent grade solvents such as acetone, isopropanol, ethanol and toluene were used as received from Sigma-Aldrich.

Spherical superparamagnetic $MnFe_2O_4$ NPs were synthesized using a protocol reported by Zeng *et al.*[17] and slightly modified by us. Briefly, 2 mmol of $Fe(acac)_3$, 1.25 mmol of $Mn(acac)_2$, 10 mmol of hexadecanediol, 6 mmol of dodecylamine, and 6 mmol of dodecanoic acid were dissolved in a round-bottom flask with 20 mL of benzyl ether. The mixture was vigorously mixed under nitrogen for 60 minutes at 140 °C, then for 120 minutes at 210 °C, and finally for 60 minutes at 300 °C. The product was washed four times with a mixture of acetone, isopropanol, and ethanol, and then dissolved in toluene. The average diameter of the obtained nanoparticles was 9 nm.

### 2.2 Functionalized cellulose sheet preparation

In order to render the sheets superparamagnetic, mother solutions of ECA in toluene were prepared with a weight ratio of 5/95 and 9/91. For the magnetic sheet, a part of this solution was mixed, under ambient conditions, with toluene solution of $MnFe_2O_4$ NPs in the weight ratio 5/95 of NPs/ECA, respectively. It is worth knowing that in order to get 1 mg of $MnFe_2O_4$ NPs, 17.4 μL of the toluene solution of $MnFe_2O_4$ NPs at a molar concentration equal to $50 \times 10^{-6}$ were needed (for this calculation the molecular weight of each nanostructure was estimated to be $1.15 \times 10^6$ amu; these data were estimated by taking into account the lattice parameter of the unit cell of $MnFe_2O_4$ and the diameter of the nanoparticle, 9 nm). Subsequently, cellulose sheets were dipped in each solution for 15 s and left to dry under ambient conditions. For the reference sample, a piece of cellulose sheet was dipped for 15 s in the initial ECA/toluene solution and left to dry.

### 2.3 Characterization

**2.3.1 Elemental analysis.** The concentrations of iron and manganese in the NP solutions and the NPs amount impregnated in the cellulose fibers were determined by elemental analysis using an ICP-AES spectrometer (iCAP 6500, Thermo). For the analysis, a small aliquot of each sample was dried and subsequently digested for 24 hours in a solution of concentrated $HCl/HNO_3$ 3 : 1 (v/v). The samples were then diluted, filtered (0.22 μm pore size syringe filter) and analyzed for ion content.

**2.3.2 Magnetic measurements.** Measurements of static magnetization were performed by a Quantum Design MPMS-XL SQUID magnetometer working in the temperature range 1.8–350 K and the magnetic field range ±5 T. Zero-field-cooled (ZFC) and field-cooled (FC) magnetizations were recorded as a function of the temperature in the presence of a 5 mT field after cooling the sample in the absence (ZFC) or in the presence (FC) of the same probe field. The magnetization (MH) curves were recorded up to ±5 T, at room (300 K) and cryogenic (2.5 K) temperatures, in the field range 0–5 T and ±5 T, respectively. All data were corrected for the diamagnetism of the solvent or cellulose support and of the sample holder which were separately determined in the same temperature and field ranges.

**2.3.3 Contact angle measurements.** Square samples were cut from the treated sheets to measure the static contact angle using a contact angle goniometer (Kruss, Germany).

**2.3.4 Microscopy imaging.** The microscopy images were acquired by an optical microscope (Carl Zeiss, Axio Scope A1) equipped with a digital camera and image processing software. Scanning electron microscopy (SEM) images were acquired by detecting back scattered electrons on a JEOL JSM-6490LA, working at 30 kV with a nitrogen pressure of 30–40 Pa to reduce sample charging. Thin cross-sectional slices (100–150 nm thick) from functionalized cellulose samples for transmission electron microscopy (TEM) imaging were cut with a Leica UC6 ultramicrotome (using wet cut at room temperature on water), after embedding the samples in epoxy resin (Epon 812), and collecting the slices on a carbon coated copper grid. All bright field TEM images were acquired on a JEOL JEM-1011 working at 100 kV.

## 3. Results and discussion

The nanocomposite solution used for the functionalization of the networks of cellulosic fibers consists of ECA monomers diluted in toluene at a percentage weight ratio of 5/95 (ECA/toluene) mixed with manganese ferrite colloidal NPs in toluene ($MnFe_2O_4$ diameter: 9 nm) at different NP/ECA ratios. The immersion of the cellulose sheets in the solution for 15 s and their subsequent removal, called dip coating technique, cause the complete wetting of the cellulose fibers followed by ECA polymerization. The polymerization is topochemical in nature, and occurs at the surface of the fiber due to the presence of the cellulosic hydroxyl groups[18] and of the environmental humidity,[19] since it is well known that the CAs present high reactivity to anions and weak bases.[19–21] The resulting poly(ethyl-2-cyanoacrylate) (PECA) polymer entraps a certain amount of superparamagnetic NPs around each cellulose fiber without changing the overall morphology of the sheets as shown in Fig. 1. In order to examine the ability of the polymer shells to trap NPs around the fibers, three freshly made solutions with percentage weight ratios 5/95, 9/91 and 25/75 of NPs/ECA were used for dip coating. The morphology for all cases looks as in Fig. 1b, *i.e.* similar to the bare cellulose sheet. Furthermore, a part of the 9/91 NPs/ECA solution was left to age for about 4 hours. The ageing increased the viscosity of the solution, since possible existence of free capping molecule traces, such as dodecylamine, in the final colloidal NP solution (see Experimental section) can highly react with the ECA monomers[20] causing the initiation of the polymerization. The dipping of the cellulose sheets in the denser solution results in the formation of a thicker nanocomposite cladding around the fibers (Fig. 1c) but, also in this case, preserving the fibers' network.

In order to define accurately the amount of the entrapped NPs in the nanocomposite shell in each case, elemental analysis of the functionalized sheets was performed using an ICP-AES spectrometer. Indeed, the per weight percentages of the entrapped NPs to the functionalized sheets, dip coated in 5/95, 9/91 and 25/75 NPs/ECA solutions, were found to be 0.59, 1.09 and

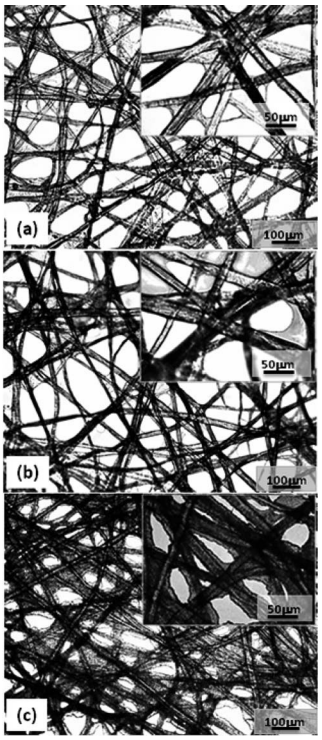


**Fig. 1** Optical microscopy representative images of cellulose sheets: (a) bare, and treated with nanocomposite formed (b) by a fresh solution 9/91 wt% of $MnFe_2O_4$ NPs/ECA in toluene, and (c) by an aged solution of 9/91 wt% $MnFe_2O_4$ NPs/ECA. Insets show higher magnifications.

2.21 wt%, respectively. The concentration ratio of the NPs between the second and the first solution is 1.8 and is preserved in the solid samples, whereas their ratios between the third and the other two solutions appear a bit higher than the respective ones of the solid samples, a difference small enough to be attributed to the experimental uncertainty. On the other hand, the 9/91 aged solution gives samples with a higher amount of entrapped NPs (1.98 wt%), compared to the freshly made one, as attributed to the already demonstrated thicker cladding, which is capable of incorporating a higher amount of NPs. Thus, by simply ageing the initial solution, the thickness of the cladding and the amount of embedded NPs can change respectively. However, in all cases the NPs/PECA nanocomposite covers each fiber by forming a functional shell, without causing an important change to the morphology of the cellulosic network.

This is also confirmed with the cross-section TEM analysis, of 100–150 nm thick cross-sectional sheet slices which were cut with an ultramicrotome after embedding the samples in epoxy resin. In particular Fig. 2 shows two individual cellulose fibers (the curled bright part with dark ripples) which are completely covered by the nanocomposite material (gray shell). When a 9/91 NPs/ECA fresh solution is used for the functionalization, the cladding is much thinner (Fig. 2a) compared with the nanocomposite cladding formed by the aged 9/91 solution (Fig. 2b), with NPs well encapsulated and homogeneously distributed in both cases. It is worth noticing that the morphology of the functionalized cellulosic networks using the 25/75 NPs/ECA solution is similar to the one shown in the Fig. 2a.

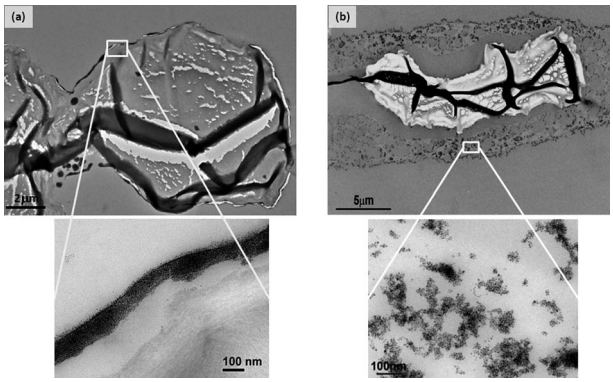


**Fig. 2** Cross-section TEM images of cellulose fibers embedded in a shell of the $MnFe_2O_4$ NPs/PECA composite, formed by 9/91 NPs/ECA (a) freshly made solution, with the inset indicating a part of the nanocomposite cladding (dark region) and the cellulose fiber on the downright part of the figure and (b) aged solution, with the inset indicating dispersed NPs in the polymer matrix.

A closer look at the modified cellulose sheets with environmental SEM imaging shows that the fibers are externally covered by agglomerates of NPs surrounding each of them (Fig. 3). The use of aged solution results in a higher amount of agglomerates with increased roughness, compared to the freshly made solution. The nanorough surface of the nanocomposite shells in combination with the waterproof character of the PECA[22] transforms the cellulosic sheets from water absorbing to hydrophobic, with static water contact angles around 120° for the samples made by fresh solutions and 140° for the samples made by the aged one. This difference can be attributed to the difference in the roughness between samples prepared by aged solutions and freshly made ones.

The magnetic properties of the modified cellulose sheets were measured and compared to those of the bare NPs in toluene solution. As shown in Fig. 4 the magnetic properties of the NPs are preserved when they are embedded in the nanocomposite shells of the cellulose fibers, with no relevant differences in the

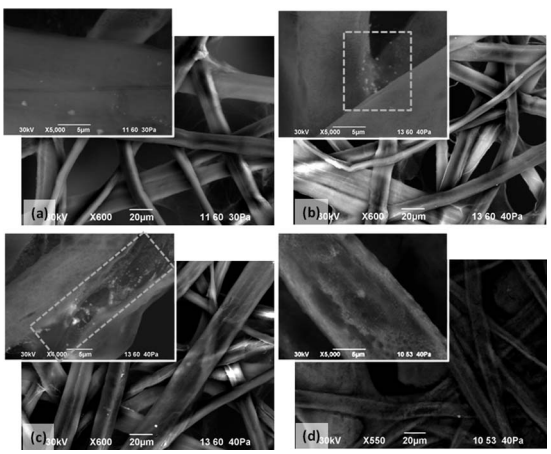


**Fig. 3** SEM images of bare (a) and functionalized cellulose sheets treated with 9/91 wt% (b), and 25/75 wt% (c) freshly made solutions. The insets show higher magnifications of the external parts of the fibers, where areas with aggregated NP structures are indicated. (d) SEM image of 9/91 wt% aged solution with the inset of a fiber covered with the nanocomposite.

shape of both zero-field-cooled and field-cooled magnetizations (ZFC/FC) and magnetization (MH) curves, at low (2.5 K) and room temperature (300 K). Specifically, the ZFC/FC magnetization curves (Fig. 4a) show that the blocking temperature, which can be identified with the temperature of the ZFC maximum, is 35–40 K for all the samples and that the difference between the blocking and irreversibility temperatures, *i.e.* the temperature at which the ZFC and FC curves collapse, is small, consistent with the very narrow size distribution of our NPs. The MH curves saturate at high fields, showing that the surface contribution to the NPs magnetic moment is negligible, as expected for 9 nm particles, and no coercivity is observed at room temperature. As suggested by the ZFC/FC behaviour, this result confirms that the NPs are in the superparamagnetic regime at room temperature for all the samples. The MH collected at low temperature (Fig. 4c) show hysteresis with a 300–350 Oe coercive field and a 0.5 reduced remanent magnetization ($M_R/M_S$) for all samples, as expected for a set of uniaxial NPs with their anisotropy axis randomly oriented. The saturation magnetization, $M_S$, of the bare NPs, normalized to the amount of magnetic material in the solution is 81 emu gr$^{-1}$ at 2.5 K and 61 emu gr$^{-1}$ at room temperature, slightly lower than the $MnFe_2O_4$ bulk value (*ca.* 80 emu gr$^{-1}$ at 300 K),[23] denoting a good level of NP crystallinity. Moreover, the $M_s$ of the entrapped NPs in each cellulose sheet, normalized to their respective amount as measured by the ICP, is about 79 emu gr$^{-1}$ at 2.5 K and *ca.* 20% lower at room temperature in all cases. This is comparable to the saturation magnetization values for the bare NPs in solution, confirming that the combination of cellulose fibers, PECA and magnetic NPs does not affect the magnetic properties of the NPs. The $M_S$ values of the different functionalized sheet samples, normalized to their weight, are 0.46, 0.86, 1.57 and 1.76 emu gr$^{-1}$ at 2.5 K, corresponding to NP concentrations 0.59%, 1.09%, 1.98% and 2.21 wt% in the functionalized sheets respectively. The $M_S$ values are reduced by 20–25% at room temperature, as observed for the NPs in toluene solution. The obtained $M_s$ values for the magnetic cellulose sheets are comparable or even higher than previous studies dealing with the magnetic functionalization of cellulosic materials using various methods, such as *in situ* NPs growth in or onto the fibers, lumen loading *etc.*, indicating the efficiency of the proposed method.[14,15,24–26]

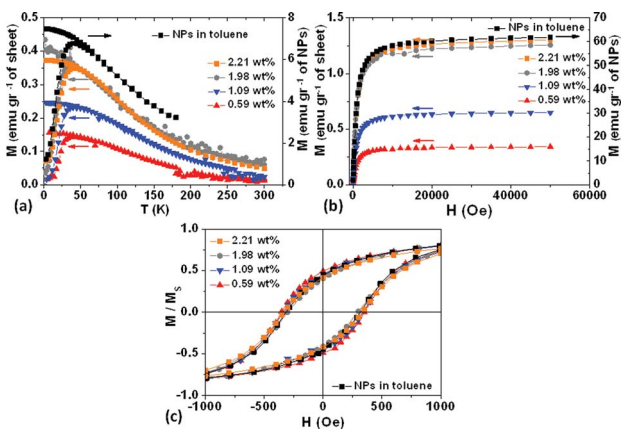


**Fig. 4** Comparison of the magnetization data obtained for the NPs dispersion in toluene and four samples of the magnetic cellulose sheets embedding different contents of magnetic NPs. (a) ZFC–FC magnetization curves; data on the solution have been acquired up to 180 K to avoid the solvent melting. (b) MH curves at room temperature (300 K). (c) Hysteresis loops measured at low temperature (2.5 K), normalized to the corresponding saturation value. The magnetization values of the functionalized sheets and of the NPs dispersion are normalized to the total weight of the cellulose sheets and to the amount of magnetic material, respectively.

The magnetization results in combination with the above-mentioned microscopic analysis confirm that the PECA acts as the medium for the encapsulation of a controlled amount of NPs around each fiber, which is proportional to their concentration in the initial solutions. Indeed, Fig. 5 shows the per weight percentage of the encapsulated NPs in the nanocomposite shells of the cellulose fibers calculated by two different ways: by calculating the ratio ($M_{s\_sheet}/M_{sNPs}$) × 100% obtained by the magnetic measurements, *i.e.* the saturation magnetization values of the functionalized sheet and of the bare NPs, and by using the NPs weight measured by the ICP with respect to the total weight of the functionalized cellulose sheet ($w_{NPs}/w_{total}$ × 100%). As shown, the relation between these two values is linear with a slope of *ca.* 1, indicating that the magnetic behaviour of the modified cellulose fibers is directly proportional to the amount of the entrapped NPs around each fiber. In all cases, the final weight percentage of the encapsulated NPs in the cellulose fiber nanocomposite network amounts to less than 2.5%.

The method presented demonstrates that the wetting of the cellulosic fiber networks by solutions of the ECA monomer carrying the functional NPs ensures that each fiber surface is effectively functionalized even when the overall NPs concentration is less than 2.5 wt% with respect to the cellulose–nanocomposite network. This is demonstrated macroscopically by transferring from one position to another the functionalized cellulose sheet using exclusively the magnetic attraction of a permanent magnet of 0.5 T. In fact, the image sequence in Fig. 6 shows that the described treatment transforms the sheet into magnetically responsive.

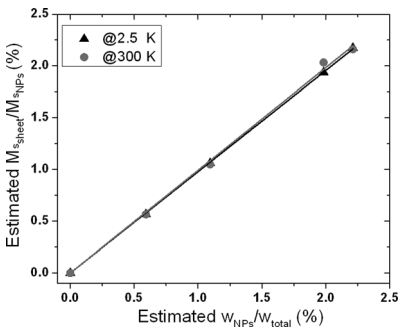


**Fig. 5** Graph showing the NPs wt% estimated by the magnetic measurements ($M_s$ of functionalized sheets/$M_s$ of the bare NPs at 2.5 K and 300 K) *versus* the NPs wt% estimated by their weight ratio in the sample (NPs quantity entrapped in the cellulose sheet obtained by ICP/weight of the total sample). The gray and black lines are the corresponding linear fits ($y = ax$) for the data at 300 K and 2.5 K respectively, indicating that the slope is *ca.* 1 for both cases (0.992 ± 0.013 and 0.978 ± 0.003 respectively).

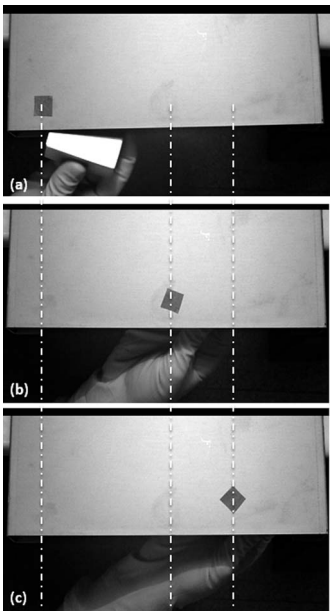


**Fig. 6** Photograph frames of the displacement of a functionalized magnetic sheet during magnetic actuation with a static magnet of 0.5 T.

## 4. Conclusions

We demonstrate a facile, inexpensive and easily scalable process for rendering any kind of commercially available cellulose sheets magnetic. The superparamagnetic NPs are entrapped in a polymer layer which forms a shell around each individual fiber, without altering their overall properties like size and shape, but providing to the sheets their superparamagnetic functional properties. Magnetic and microscopy studies proved that the amount of the NPs entrapped around the fibers depends on their initial concentration in the monomer/NPs solution and on the density of the overall solution, proving thus the ability of the monomer to polymerize around the fibers forming a shell where a controlled amount of NPs can be trapped. The modified cellulose sheets attain magnetic responsivity features and furthermore become water repellent. These very important findings open up the way for the use of cellulose sheets in sensors and fluidics applications with huge economic benefits.

## Acknowledgements

The authors thank Ms Roberta Ruffilli of Istituto Italiano di Tecnologia (IIT) for helping with sample preparation for the TEM and SEM analysis.

## References

1 H. Gullapalli, V. S. M. Vemuru, A. Kumar, A. Botello-Mendez, R. Vajtai, M. Terrones, S. Nagarajaiah and P. M. Ajayan, *Small*, 2010, **6**, 1571.
2 D. Nilsson, T. Kugler, P.-O. Svensson and M. Berggren, *Sens. Actuators, B*, 2002, **86**, 193.
3 Z. Ding, P. Wei, G. Chitnis and B. Ziaie, *J. Microelectromech. Syst.*, 2011, **20**, 59.
4 W. Lim, E. A. Douglas, S.-H. Kim, D. P. Norton, S. J. Pearton, F. Ren, H. Shen and W. H. Chang, *Appl. Phys. Lett.*, 2009, **94**, 072103.
5 L. Hua, J. W. Choia, Y. Yanga, S. Jeongb, F. La Mantiaa, L.-F. Cuia and Y. Cuia, *Proc. Natl. Acad. Sci. U. S. A.*, 2009, **106**, 21490.
6 X. Liu, M. Mwangi, X. J. Li, M. O'Brien and G. M. Whitesides, *Lab Chip*, 2011, **11**, 2189.
7 W. Zhao and A. van den Berg, *Lab Chip*, 2008, **8**, 1988.
8 B. Balu, A. D. Berry, D. W. Hess and V. Breedveld, *Lab Chip*, 2009, **9**, 3066.
9 C. H. Chia, S. Zakaria, S. Ahamd, M. Abdullah and S. M. Jani, *Am. J. Appl. Sci.*, 2006, **3**, 1750.
10 S. Zakaria, B. H. Ong and T. G. M. van de Ven, *Colloids Surf., A*, 2004, **251**, 31.
11 S. Zakaria, B. H. Ong and T. G. M. van de Ven, *Colloids Surf., A*, 2004, **251**, 1.
12 J. Shen, Z. Song, X. Qian and Y. Ni, *Ind. Eng. Chem. Res.*, 2011, **50**, 661.
13 A. C. Small and J. H. Johnston, *J. Colloid Interface Sci.*, 2009, **331**, 122.
14 A. Walther, J. V. I. Timonen, I. Díez, A. Laukkanen and O. Ikkala, *Adv. Mater.*, 2011, **23**, 2924.
15 S. Liu, L. Zhang, J. Zhou and R. Wu, *J. Phys. Chem. C*, 2008, **112**, 4538.
16 R. T. Olsson, M. A. S. Azizi Samir, G. Salazar-Alvarez, L. Belova, V. Strom, L. A. Berglund, O. Ikkala, J. Nogues and U. W. Gedde, *Nat. Nanotechnol.*, 2010, **5**, 584.
17 H. Zeng, P. M. Rice, S. X. Wang and S. H. Sun, *J. Am. Chem. Soc.*, 2004, **126**, 11458.
18 M. Alava and K. Niskanen, *Rep. Prog. Phys.*, 2006, **69**, 669.
19 S. V. Doiphode, D. H. Reneker and G. G. Chase, *Polymer*, 2006, **47**, 4328.
20 R. B. Paul, J. M. Kelly, D. C. Pepper and C. Long, *Polymer*, 1997, **38**, 2011.
21 L. Zhang, N. Zhao, X. Li, Y. Long, X. Zhang and J. Xu, *Soft Matter*, 2011, **7**, 4050.
22 I. S. Bayer, D. Fragouli, A. Attanasio, B. Sorce, G. Bertoni, R. Brescia, R. Di Corato, T. Pellegrino, M. Kalyva, S. Sabella, P. P. Pompa, R. Cingolani and A. Athanassiou, *ACS Appl. Mater. Interfaces*, 2011, **3**, 4024.
23 M. Schieber, in *Experimental Magnetochemistry: Non-Metallic Magnetic Materials*, North-Holland Publishing, Amsterdam, 1967.
24 S. Zakaria, B. H. Ong, S. H. Ahmad, M. Abdullah and T. Yamauchi, *Mater. Chem. Phys.*, 2005, **89**, 216.
25 J. Zhou, R. Li, S. Liu, Q. Li, L. Zhang, L. Zhang and J. Guan, *J. Appl. Polym. Sci.*, 2009, **111**, 2477.
26 C. Katepetch and R. Rujiravanit, *Carbohydr. Polym.*, 2011, **86**, 162.

 